SLAC-PUB-11279

A STUDY OF SEMILEPTONIC B DECAYS AND OF LEPTON FLAVOR VIOLATING τ DECAYS AT *BABAR*

Olga Igonkina (representing the *BABAR* Collaboration)
University of Oregon, Eugene, OR 97403, USA

Abstract

The study of the semileptonic B decays at *BABAR* is presented. The results shown include measurements of the moments of hadronic-mass and electron-energy of the decay $B \to X_c\,\ell\nu$; a determination of the $|V_{cb}|$ CKM matrix element and other heavy quark parameters from a simultaneous fit to the moments using kinetic scheme of Operator Product Expansion; a measurement of the inclusive branching fraction of $B \to X_u\,\ell\nu$ and determination of $|V_{ub}|$. The most resent *BABAR* search for the lepton flavor violating decays $\tau \to \ell\ell\ell$ is presented as well.

Contributed to 39th Rencontres de Moriond on QCD and High-Energy Hadronic Interactions, 03/28/2004--4/4/2004, La Thuile, Italy

Work supported in part by Department of Energy contract DE-AC02-76SF00515

SLAC, Stanford Univesity, Stanford, CA 94309

1 Introduction

This talk summarizes recent results of the study of the semileptonic B meson decays from the *BABAR* experiment as well as a search of lepton flavor violating τ decays to 3 charged leptons. The measurements presented here are based on data collected with the *BABAR* detector at the PEP-II asymmetric energy e^+e^- collider near the $\Upsilon(4S)$ resonance. The *BABAR* detector is described in detail elsewhere [1]. Charged-particle (track) momenta are measured with a 5-layer double-sided silicon vertex tracker and a 40-layer drift chamber inside a 1.5-T superconducting solenoidal magnet. An electromagnetic calorimeter consisting of 6580 CsI(Tl) crystals is used to identify electrons and photons, a ring-imaging Cherenkov detector and energy loss in the drift chambers are used to identify charged hadrons, and the instrumented magnetic flux return is used to identify muons.

The talk is structured in the following way. Section 2 presents the study of the inclusive Cabibbo-favored decays $B \to X_c\,\ell\nu$: the measurement of the moments of electron energy distribution; the measurement of the moments of the hadronic mass distribution and the of determination of $|V_{cb}|$ CKM matrix element and heavy quark parameters in the combined fit of the moments with no external parameters within Operator Product Expansion framework. Section 3 concentrates on the measurement of the branching fraction of the inclusive Cabibbo-suppressed decays $B \to X_u\,\ell\nu$ and determination of the $|V_{ub}|$ CKM matrix element. Section 4 describes a search of lepton flavor violating τ decays $\tau \to \ell\ell\ell$, where $\ell = e, \mu$.

2 Cabibbo-favored decays $B \to X_c\,\ell\nu$

The precise measurement of the CKM matrix element $|V_{cb}|$ is a necessary component to constrain and check the validity of the Standard model (SM). While there are many methods to extract $|V_{cb}|$ from the inclusive and exclusive Cabibbo-favored decays of B mesons [2], the combined fit of the distribution of the lepton energy (E_ℓ) and the invariant mass of the hadron system (M_X) from inclusive $B \to X_c\,\ell\nu$ decays allows the most precise determination of the $|V_{cb}|$ with no external constrains involved. The $B \to X_c\,\ell\nu$ rate can be expressed as

$$\Gamma_{c\ell\nu} = \frac{G_F^2 m_b^5}{192\pi^3}|V_{cb}|^2(1+A_{ew})A_{pert}A_{nonpert} \cong |V_{cb}|^2 f_{OPE}(a_i), \qquad (1)$$

where A_{ew}, A_{pert} and $A_{nonpert}$ are electro-weak, perturbative and non-perturbative contributions. The function $f_{OPE}(a_i)$ is calculated using Operator Product Expansion [3] and has six parameters a_i within order α_s^2 and $1/m_b^3$ [4]. Heavy quark parameters a_i can be extracted from the E_ℓ and M_X moments

(M_n^ℓ, M_n^X) using the same framework [5]:

$$M_n^\ell, M_n^X = < Y^n > (E_{cut}) = \left. \frac{\int (Y - Y^0)^n \frac{d\Gamma}{dY}\, dY}{\int \frac{d\Gamma}{dY}\, dY} \right|_{E_\ell > E_{cut}} \cong f'_{OPE}(a_i), \quad (2)$$

where the lower cut on lepton energy E_{cut} is introduced to avoid infra-red divergence in the calculations. The calculations of $f_{OPE}(a_i)$ and $f'_{OPE}(a_i)$ can be done using different *mass schemes*, although the resulting $|V_{cb}|$ and the decay rate are independent of the scheme used.

The measurement of the electron-energy moments was done using a sample of 47.4 fb^{-1}, while the analysis of the hadronic invariant mass moments is based on 82 fb^{-1} sample collected at $\Upsilon(4S)$ resonance.

2.1 Measurement of the electron-energy moments

The measurement of the electron energy spectrum is performed using a di-electron sample where one (*signal*) electron has momentum $p^* > 0.5$ GeV/c in the $\Upsilon(4S)$ rest frame and another (*tag*) electron has momentum of $1.4 < p^* < 2.3$ GeV/c. The unlike-sign and like-sign lepton pairs are considered separately. In the absence of $B^0\bar{B}^0$ mixing, the former consist of two primary electrons from the semileptonic B decays while the latter are due to the presence of primary and secondary electrons from semileptonic D meson decays. Backgrounds are suppressed by cuts on the track multiplicity, the angle between two electrons and on their invariant mass as described in [6]. Fig.1 shows the electron momentum spectra superimposed with estimates for the background contribution from the continuum background, photon conversions, Dalitz decays, the events with hadrons misidentified as electron as estimated from Monte Carlo (MC) and data control samples. The electron spectra are corrected for electron identification efficiency and radiative losses. The irreducible backgrounds from decays of τ leptons, charmed mesons and $\psi \to e^+e^-$ with only one lepton identified are estimated using a MC simulation.

To account for $B^0\bar{B}^0$ mixing, the number of primary ($N_{B\to Xe\nu}$) and secondary ($N_{B\to X_c\to Xe\nu}$) electrons are extracted from the unlike-sign (N^{+-}) and like-sign ($N^{\pm\pm}$) pairs as

$$\begin{aligned} N^{+-} &= (1-\chi)\cdot N_{B\to Xe\nu} + \chi \cdot N_{B\to X_c\to Xe\nu} + N_{bgr}^{+-} \\ N^{\pm\pm} &= \chi \cdot N_{B\to Xe\nu} + (1-\chi)\cdot N_{B\to X_c\to Xe\nu} + N_{bgr}^{\pm\pm}, \end{aligned} \quad (3)$$

where χ is the $B^0\bar{B}^0$ mixing parameter multiplied by the fraction of the neutral B pairs [2] and N_{bgr} is an estimated background level. The obtained spectrum of primary electrons is shown on Fig. 2.

The distribution of leptons from $B \to X_c\,\ell\nu$ is obtained by subtracting from $B \to X\ell\nu$ the contribution of the charmless semileptonic $B \to X_u\,\ell\nu$

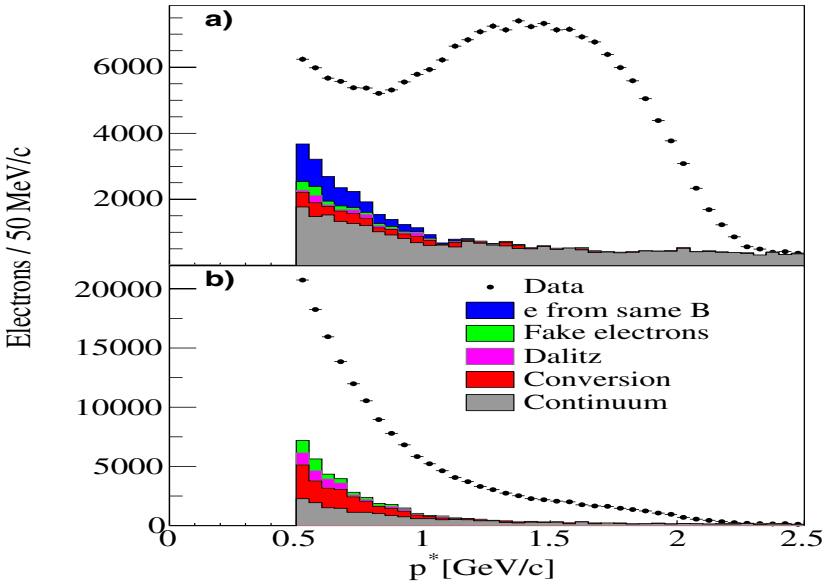

Figure 1: *Measured momentum spectrum (points) and estimated backgrounds (histograms) for electron candidates in* (*a*) *the unlike-sign sample and* (*b*) *the like-sign sample.*

decays. The latter is estimated using the MC assuming $\mathcal{B}(B \to X_u\,\ell\nu) = (2.2 \pm 0.5) \times 10^{-3}$ [7].

The electron-energy moments are determined as

$$\bar{M}_n^E = \sum_k p_k^n N_{B\to X_c\,\ell\nu}^k / \sum_k N_{B\to X_c\,\ell\nu}^k, \tag{4}$$

where k runs over all bins above the energy E_{cut} and p_k are the bin centers for $n = 1$ and the bin centers shifted by $\bar{M}_1^E$ for $n = 2, 3$. These moments are then transformed into M_n^ℓ moments by correcting for the movement of the B mesons in the center-of-mass frame (CM). The M_n^ℓ moments as a function of E_{cut} are shown in the lower row of Fig. 3. Note that the measurements are highly correlated. The numerical results and full correlation matrix can be found in ref. [6]. This is a first measurement of M_n^ℓ moments as a function of the cut on the lepton energy. The results are consistent with measurements of the moments done by CLEO [8] and by DELPHI [9].

Using the background corrected number of tag electrons and the efficiency to select a sample with one electron, we obtain the partial branching fraction

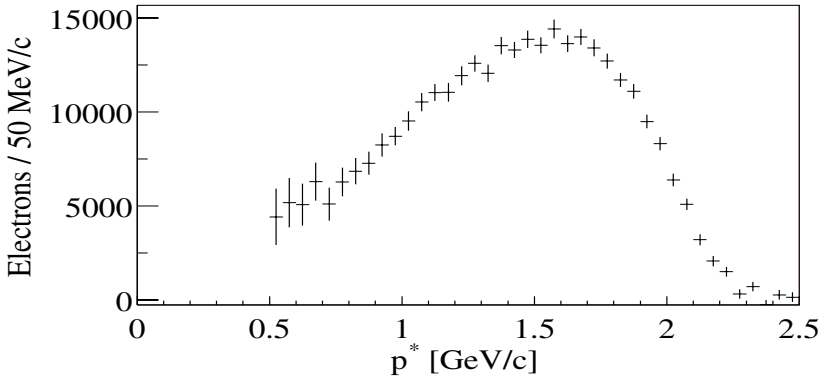

Figure 2: *Electron momentum spectrum from $B \to Xe\nu(\gamma)$ decays in the $\Upsilon(4S)$ frame after correction for efficiencies and bremsstrahlung, with combined statistical and systematical errors.*

$\mathcal{B}(B \to Xe\nu(\gamma))|_{E_{cut}>0.6\ GeV} = (10.36 \pm 0.06_{stat} \pm 0.23_{sys})\%$. This result is consistent with our previous measurement [10] with an overall error improved by 25%.

2.2 Measurement of the hadronic-mass moments

The analysis of the hadronic-mass moments uses $\Upsilon(4S) \to B\bar{B}$ events with one fully reconstructed hadronic B decay (B_{rec}) [7] and a second recoiling B meson with one and only one lepton (electron or muon) in the final state. While this approach results in a low overall event selection efficiency, it allows the determination of the momentum, charge and flavor of the B mesons. The hadronic system X in the decay $B \to X\ell\nu$ is reconstructed from charged tracks and energy depositions in the calorimeter that are not associated with the B_{rec} candidate or the charged lepton. Charged candidates are assigned either $K^{\pm}$ or $\pi^{\pm}$ mass based on particle identification information. The missing momentum p_ν in the event is required to be greater than 0.5 GeV/c. The mass of the hadronic system M_X is determined by a kinematic fit that imposes four-momentum conservation, equality of the masses of two B mesons and constrains $p_\nu^2 = 0$. The resulting mass resolution is 350 MeV/c^2.

The background contribution is estimated from the fit of the observed beam-energy-substituted mass m_{ES} in several bins of M_X. The m_{ES} is defined as $\sqrt{s/4 - \vec{p}_B^{\,2}}$ where $\sqrt{s}$ is the total energy in CM and $\vec{p}_B$ is the B_{rec} CM momentum. Figure 4a shows the M_X distribution after combinatorial back-

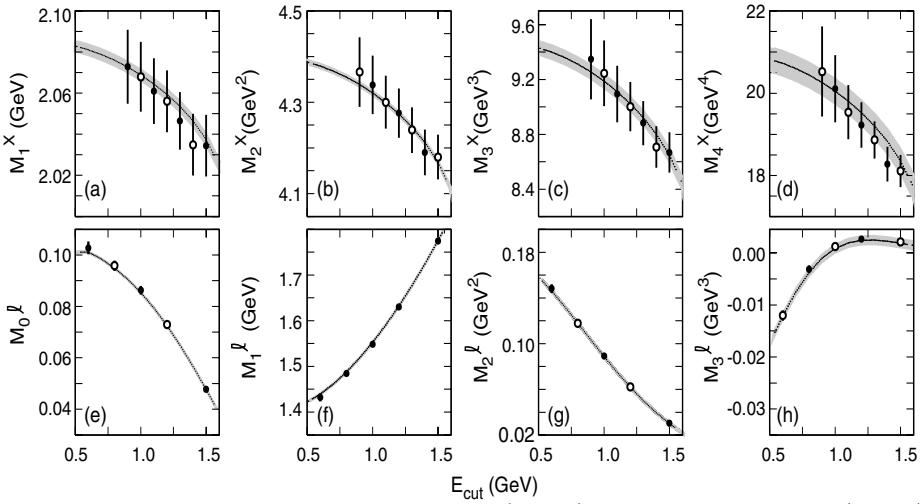

Figure 3: *The measured hadronic-mass* $(a-d)$ *and electron-energy* $(e-h)$ *moments as a function of the cut-off energy,* E_{cut}*, compared with the result of the simultaneous fit (line), with the theoretical uncertainties* [3] *indicated as shaded bands. The solid data points mark the measurements included in the fit. The vertical bars indicate the experimental errors. Moment measurements for different* E_{cut} *are highly correlated.*

ground subtraction. Due to incomplete detector acceptance the observed mass distribution is distorted with respect to the true mass distribution. Fig. 4b shows the linear relation between the reconstructed M_n^X moments and the true $M_n^{X,true}$ values estimated from MC, which is also validated on data using sample of partially reconstructed $D^{*+} \to D^0\pi^+$ decays. The observed linear dependence is used to obtain unbiased M_n^X moments. In this way, the results do not depend on assumptions for the branching fractions and mass distributions for high mass hadronic states. The hadronic-mass moments obtained after background subtraction, correction for $B \to X_u\,\ell\nu$ decays and reconstruction bias are presented in the upper row of the Fig. 3. The points are highly correlated. The numerical results can be found in ref. [11] as well as all uncertainties and correlation coefficients.

2.3 Determination of the Branching fraction of $B \to X_c\,\ell\nu$ and of $|V_{cb}|$ CKM matrix element

To extract the $|V_{cb}|$ CKM element from the fit to the electron-energy and hadronic-mass moments one can use the OPE kinetic scheme calculations of

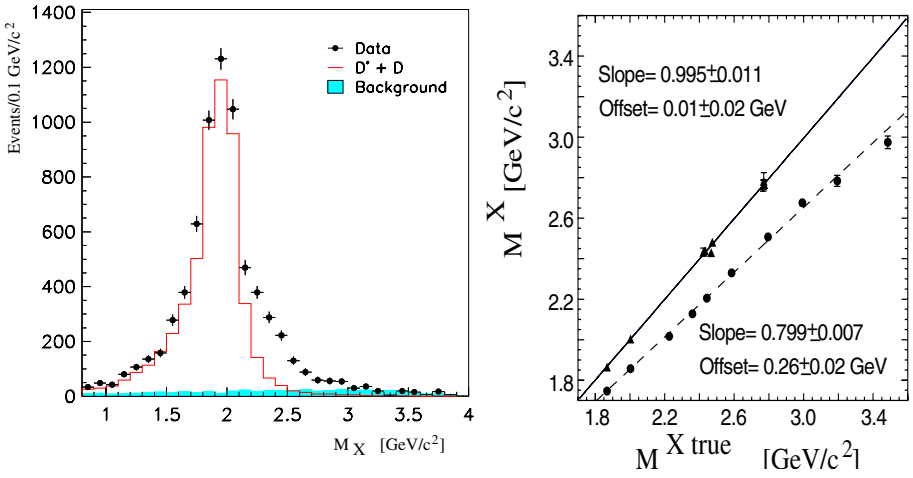

Figure 4: (*a*) M_X *distributions after subtraction of the combinatorial background in the* B_{rec} *sample, for* $p^*_{min} = 0.9$ *GeV. The Monte Carlo prediction for decays to* D *and* D^* *is indicated by the open histogram, the small residual background by the solid histogram.* (*b*) *Results of the* $< M_X >$ *calibration procedure. The calibration data and fit results are shown by the lower dashed like (circles), the verification by the upper solid line (triangles).*

the eq. 1 and 2 [5], where

$$|V_{cb}| = \sqrt{\frac{\mathcal{B}_{B\to X_c\,\ell\nu}}{\tau_B}} \cdot [C_0 + \sum C_i \cdot (a_i - a_i^0)], \qquad (5)$$

where the parameters a_i are the masses of b and c quarks m_b, m_c (at leading order); the expectation values of the kinetic μ_π^2 and chromomagnetic μ_G^2 dimension-five operators (at $\mathcal{O}(1/m_b^2)$) and the expectations values of the Darwin ρ_D^3 and spin-orbit ρ_{LS}^3 dimension-six operators (at $\mathcal{O}(1/m_b^3)$). C_i are numerical coefficients; a_i^0 are *a priori* estimates of these parameters and $\tau_B = (1.608 \pm 0.012)$ ps is average lifetime of B mesons produced at the $\Upsilon(4S)$. The calculations for M_n^X and M_n^ℓ moments in form similar to eq. 5 is available in ref. [5] up to order α_s and α_s^2, respectively. These linear equations are used to determine heavy quark parameters a_i, total branching fraction $B \to X_c\,\ell\nu$ and $|V_{cb}|$ from the simultaneous χ^2 fit to the measured moments and the partial branching fraction, all as a function of the cut-off lepton energy E_{cut}. Since many of the individual moments are highly correlated only the set of them for which the correlation coefficients do not exceed 95% is selected. The fit takes into account the statistical and systematic uncertainties, correlations between measurements and uncertainties of the calculations for the individual moments.

The resulting fit describes the data very well as shown in Fig. 3. From the fit we obtain [12]:

$$\begin{aligned} |V_{cb}| &= (41.4 \pm 0.4_{exp} \pm 0.4_{OPE} \pm 0.6_{th})\, 10^{-3}, \\ \mathcal{B}_{B\to X_c\,\ell\nu} &= (10.61 \pm 0.16_{exp} \pm 0.06_{OPE})\%, \\ m_b(1\mathrm{GeV}) &= (4.61 \pm 0.05_{exp} \pm 0.04_{OPE} \pm 0.02_{th})\mathrm{GeV}, \\ (m_b - m_c)(1\mathrm{GeV}) &= (3.436 \pm 0.025_{exp} \pm 0.018_{OPE} \pm 0.010_{\alpha_s})\mathrm{GeV}. \end{aligned}$$

The errors given stand for uncertainties associated with the measurement (*exp*), with the linearized expression (*OPE*) and with theoretical calculation (*th*) which includes various perturbative and higher order non-perturbative corrections. The full table including correlation matrix can be found in [12].

The fit results are fully compatible with independent estimates of $\mu_G^2 = (0.35 \pm 0.07)$ GeV^2, based on $B^* - B$ mass splitting [5] and of $\rho_{LS}^3 = (-0.15 \pm 0.10)$ GeV^2 from the heavy-quark sum rule [13]. The Fig. 5 shows $\Delta\chi^2 = 1$ ellipses for $|V_{cb}|$ versus m_b for a fit to all moments and separate fits to electron-energy moments and hadronic-mass moments, but including the partial branching fractions in both. The lepton-energy and hadronic-mass moments have slightly different sensitivity to the fit parameters, but the results for separate fits, $|V_{cb}| = (41.4 \pm 0.7) \times 10^{-3}$ and $|V_{cb}| = (41.6 \pm 0.8) \times 10^{-3}$ are fully compatible with each other and with the global fit to all moments. Since the expansion for the two sets of moments is sensitive to different theoretical uncertainties and assumptions, in particular the difference in the treatment of the perturbative corrections, the observed consistency of separate fits indicates that such differences are small compared with experimental and assumed theoretical uncertainties.

The results on $|V_{cb}|$ is in agreement with previous measurements using OPE either for a different mass scheme and with fixed terms of $\mathcal{O}(1/m_b^3)$ [8] or for the kinetic-mass scheme, but with external constrains on almost all OPE parameters [9] as well as with an analysis combining both of these measurements [14].

3 Cabibbo-suppressed decays $B \to X_u\,\ell\nu$

To check the consistency of the Standard Model the measurement of parameter $|V_{ub}|$ is equally important as the measurement of $|V_{cb}|$. However, the branching fraction of $B \to X_u\,\ell\nu$ is 50 times smaller than $B \to X_c\,\ell\nu$ which makes it difficult to get a sample free of the Cabibbo-favored contribution.

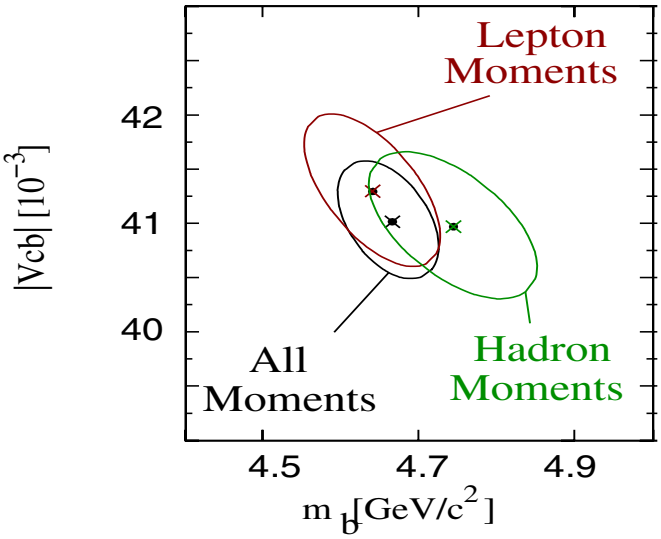

Figure 5: *Fit results (crosses) with contours corresponding to* $\Delta\chi^2 = 1$ *for* m_b *versus* $|V_{cb}|$*, separately for fits using hadronic-mass, the electron-energy, and all moments.*

3.1 Measurement of the Branching fraction $B \to X_u\,\ell\nu$

The *BABAR* analysis of the $B \to X_u\,\ell\nu$ decays presented here is done with the same sample of fully reconstructed hadronic-tag B decays as the measurement of the $B \to X_c\,\ell\nu$ hadronic-mass moments. The method for the calculation of the hadronic mass is also similar to $B \to X_c\,\ell\nu$ hadronic-mass moments analysis. To select $B \to X_u\,\ell\nu$ candidates exactly one charged lepton with momentum $p^* > 1$ GeV/c is required, the total charge in the event must be equal to zero and the missing mass must be consistent with zero ($m^2_{miss} < 0.5\mathrm{GeV}^2/\mathrm{c}^4$). Events with charged or neutral kaons in the recoil B are removed from consideration as well as $\bar{B} \to D^{*+}\ell^-\bar{\nu}$ decays which are characterized by the presence of slow π^+.

We determine the ratio R_u of the $\mathcal{B}(B \to X_u\,\ell\nu)$ to the total semileptonic B decays rate as the number of $B \to X_u\,\ell\nu$ candidates with $M_X < 1.55$ GeV/c^2 (N_u) divided by the number of events with at least one charged lepton (N_{sl}) and corrected for the selection efficiency ratio. The number N_u is extracted from the M_X distribution by a χ^2 fit to the sum of three contributions: the signal, the background from $B \to X_c\,\ell\nu$ and the background from other sources such as misidentified leptons, secondary τ and charm decays (see Fig. 6a). To minimize the model dependence the first bin covers the region up to $M_X = 1.55$ GeV/c^2. N_{sl} is derived from the fit to m_{ES} distribution shown in Fig. 6b where the signal peaks at B meson mass. The residual background in N_{sl} from misidentified leptons and semileptonic charm decays is subtracted. R_u

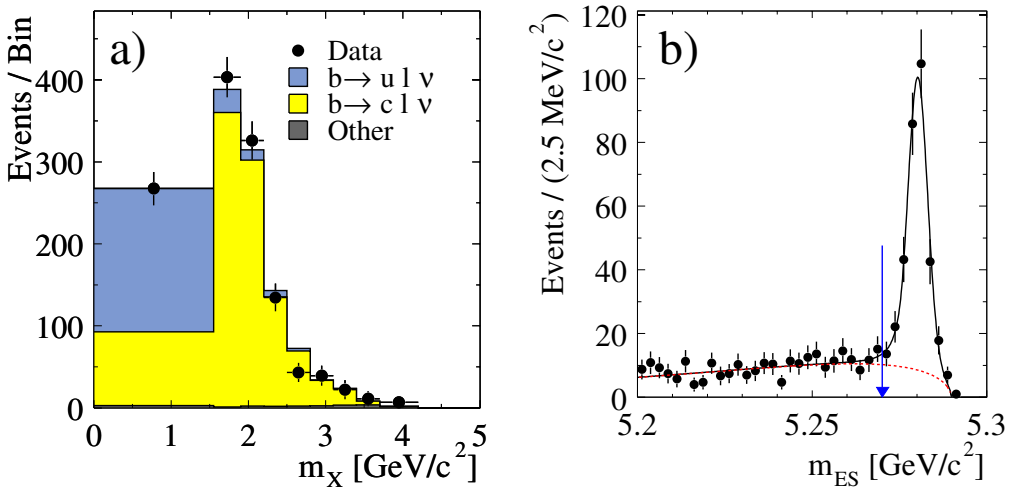

Figure 6: (*a*) *The data (points) and fit components (shaded histograms) of* M_X *distribution for* $B \to X\ell\nu$*; (b) Fit to the* m_{ES} *distribution for the sample after all requirements and with* $M_X < 1.55$ GeV/c^2*. The arrow indicates the lower limit of the signal region.*

is found to be equal to $(2.06 \pm 0.25_{stat} \pm 0.23_{sys} \pm 0.36_{th})\,10^{-2}$ which gives $\mathcal{B}(B \to X_u\,\ell\nu) = (2.24 \pm 0.27_{stat} \pm 0.26_{sys} \pm 0.39_{th})\,10^{-3}$ when multiplied with $B \to X\ell\nu$ branching fraction from ref. [10]. The uncertainties given are statistical, systematic (experimental plus signal and background modeling) and theoretical, respectively. The details of the measurement can be found in ref. [7].

3.2 Determination of the $|V_{ub}|$ matrix element

Within the OPE framework $|V_{ub}|$ is estimated from the measurement of $\mathcal{B}(B \to X_u\,\ell\nu)$ as:

$$|V_{ub}| = 0.00445 \cdot \sqrt{\frac{\mathcal{B}(b \to u\ell\nu)}{0.002}\frac{1.55\text{ps}}{\tau_b}} \cdot (1 \pm 0.056_{th}) \qquad (6)$$

(see ref. [2]) where the uncertainty given does not include a possible contribution from parton-hadron duality. Using the measurement of $\mathcal{B}(B \to X_u\,\ell\nu)$ given above we obtain [7] $|V_{ub}| = (4.62 \pm 0.28_{stat} \pm 0.27_{sys} \pm 0.40_{MC} \pm 0.26_{th})\,10^{-3}$, where the uncertainties are statistical, systematic, the uncertainty

in the signal efficiency and the extrapolation of R_u to the full M_X range and uncertainty from eq. 6. The result is consistent with previous inclusive measurements [15], but based on a sample with larger phase-space acceptance and higher purity.

4 Search for lepton flavor violating decays $\tau \to \ell\ell\ell$

Among other searches for physics beyond the Standard Model, *BABAR* has performed studies of lepton flavor violating tau decays $\tau \to \ell\ell\ell$ ($\ell = e, \mu$) using the data sample of 91.5 fb^{-1}. Even with the inclusion of neutrino oscillation into the SM, the branching fractions of $\tau \to \ell\ell\ell$ are expected to be of the order of 10^{-14} [16], while many SM extensions and SUSY theories predict values comparable with modern experimental sensitivity [17].

In the analysis, the event is required to have 1-3 topology, i.e. 4 tracks with net zero charge pointing towards a common region, with one track separated from the others by at least 90^o in the CM. All tracks on the 3-prong side must be identified as a lepton, muon of electron, with invariant mass (m_{rec}) close to the mass of tau $m_\tau = 1.777$ and a measured energy in the CM (E^{CM}_{rec}) equal to $\sqrt{s}/2$. The 6 modes under consideration are contaminated by QED (Bhabha and di-muon), generic $\tau\tau$ and $q\bar{q}$ events. The cuts to suppress these backgrounds consist of a veto on the 1-prong lepton identification, a cut on the momentum of the 1-prong charged particle, on the angle between 1- and 3-prong momenta and cuts on the number of photon and Kaon candidates on the 3-prong side as detailed in ref. [18]. The selection efficiency for signal events (ε) depends on the decay mode and varies from 7 to 12% as shown in Table 1.

The selected events are studied using $\Delta M = m_{rec} - m_\tau$ and $\Delta E = E^{CM}_{rec} - E^{CM}_{beam}$ variables. The backgrounds remaining after selection have distinctive distribution in the (ΔM,ΔE) plane: $q\bar{q}$ tend to populate the plane uniformly, while QED backgrounds are restricted to a narrow band at positive values of ΔE, and $\tau\tau$ are restricted to negative values of both ΔM and ΔE. A negligible two-photon background remains. The background rates for each decay mode are estimated by fitting a set of probability density functions (*PDFs*) to the observed data in (ΔM, ΔE) in the region surrounding a signal region (*SB*) indicated with a box in Fig. 7. The parameters of the PDFs are determined from MC and data control samples. The expected number of background events in the SB is calculated from the PDFs and is compared with observed number of events (see Table. 1).

No signal is observed in any decay mode (see Fig. 7) and an upper limit on branching fractions ($\mathcal{B}^{90}_{UL}$) is estimated as:

$$\mathcal{B}^{90}_{UL} = N^{90}_{UL}/(2\varepsilon N_{\tau\tau}) \tag{7}$$

Table 1: *Efficiency estimates (ε), number of expected background events ($N_{\rm bgd}$), number of observed events ($N_{\rm obs}$), and branching fraction upper limits for each $\tau \to \ell\ell\ell$ decay mode.*

Decay mode	$e^-e^+e^-$	$\mu^+e^-e^-$	$\mu^-e^+e^-$
Efficiency [%]	7.3 ± 0.2	11.6 ± 0.4	7.7 ± 0.3
$N_{\rm bgd}$	1.51 ± 0.11	0.37 ± 0.08	0.62 ± 0.10
$N_{\rm obs}$	1	0	1
$\mathcal{B}^{90}_{\rm UL}$	2.0×10^{-7}	1.1×10^{-7}	2.7×10^{-7}
Decay mode	$e^+\mu^-\mu^-$	$e^-\mu^+\mu^-$	$\mu^-\mu^+\mu^-$
Efficiency [%]	9.8 ± 0.5	6.8 ± 0.4	6.7 ± 0.5
$N_{\rm bgd}$	0.21 ± 0.07	0.39 ± 0.08	0.31 ± 0.09
$N_{\rm obs}$	0	1	0
$\mathcal{B}^{90}_{\rm UL}$	1.3×10^{-7}	3.3×10^{-7}	1.9×10^{-7}

where N^{90}_{UL}, $N_{\tau\tau}$ are the 90% confidence upper limit for the number of signal events for the given mode and the number of $\tau\tau$ pairs, respectively. The N^{90}_{UL} is estimated using Counsins, Highland method [19] which includes the estimated systematic uncertainties on the signal efficiency (3-7%), on the expected background (8-33%) and on the $N_{\tau\tau}$ (2.4%).

5 References

References

1. B. Aubert *et al.* [*BABAR* Collaboration], Nucl. Instrum. Meth. **A479** 1 (2002)
2. K. Hagiwara *et al*, Phys. Rev. **D66**, 010001 (2002)
3. M. Voloshin and M. Shifman, Sov. J. Nucl. Phys. **41**, 120 (1985); J. Chay, H. Georgi, and B. Grinstein, Phys. Lett. **B247**, 399 (1990); I. I. Bigi, and N. Uraltsev, Phys. Lett. **B280**, 271 (1992).
4. I. I. Bigi, M. Shifman, N. Uraltsev, and A. Vainshtein, Phys. Rev. **D56**, 4017 (1997). D. Benson, I. I. Bigi, T. Mannel, and N. Uraltsev, Nucl. Phys. **B665**, 367 (2003).
5. P. Gambino and N. Uraltsev, Eur. Phys. J. C **34**, 181 (2004)
6. B. Aubert *et al.* [*BABAR* Collaboration], Phys. Rev. D **69**, 111104 (2004)

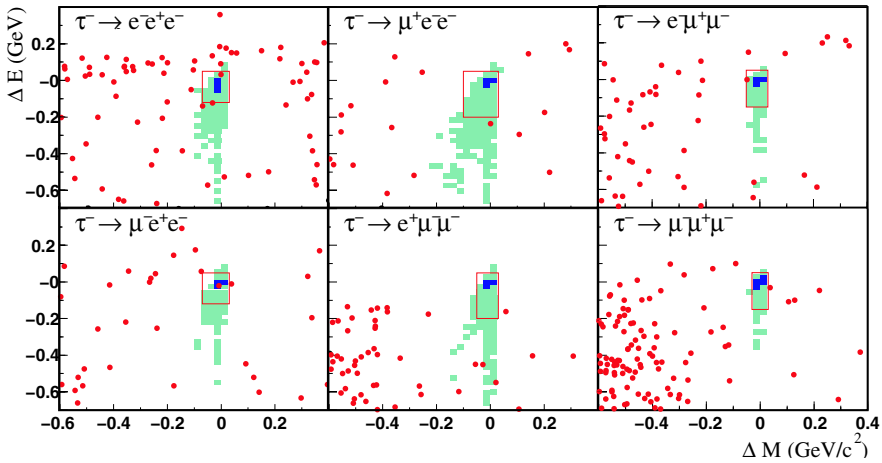

Figure 7: *Observed data shown as dots in the* $(\Delta M, \Delta E)$ *plane and the boundaries of the signal region for each decay mode. The dark and light shading indicates contours containing 50% and 90% of the selected MC signal events, respectively.*

7. B. Aubert *et al.* [*BABAR* Collaboration], Phys. Rev. Lett. **92**, 071802 (2004)

8. A. H. Mahmood *et al.* (CLEO Collaboration), Phys. Rev. D **67**, 072001 (2003)

9. M. Battaglia *et al.*, Phys. Lett. B **556**, 41 (2003)

10. B. Aubert *et al.* [*BABAR* Collaboration, Phys. Rev. D **67**, 031101 (2003)

11. B. Aubert *et al.* [*BABAR* Collaboration], Phys. Rev. D **69**, 111103 (2004)

12. B. Aubert *et al.* [*BABAR* Collaboration], Phys. Rev. Lett. **93**, 011803 (2004)

13. I. I. Y. Bigi, M. A. Shifman and N. Uraltsev, Ann. Rev. Nucl. Part. Sci. **47**, 591 (1997)

14. C. W. Bauer, Z. Ligeti, M. Luke and A. V. Manohar, Phys. Rev. D **67**, 054012 (2003)

15. R. Barate *et al.* [ALEPH Collaboration], Eur. Phys. J. C **6**, 555 (1999); M. Acciarri *et al.* [L3 Collaboration], Phys. Lett. B **436**, 174 (1998). P. Abreu *et al.* [DELPHI Collaboration], Phys. Lett. B **478**, 14 (2000)

G. Abbiendi *et al.* [OPAL Collaboration], Eur. Phys. J. C **21**, 399 (2001)
A. Bornheim *et al.* [CLEO Collaboration], Phys. Rev. Lett. **88**, 231803 (2002)

16. X. Y. Pham, Eur. Phys. J. C **8**, 513 (1999)

17. E. Ma, Nucl. Phys. Proc. Suppl. **123**, 125 (2003)

18. B. Aubert *et al.* [*BABAR* Collaboration], Phys. Rev. Lett. **92**, 121801 (2004)

19. R. D. Cousins and V. L. Highland, Nucl. Instrum. Meth. A **320**, 331 (1992).